Intrinsic Viscosity of Oligo- and Poly(methyl methacrylate)s

Yasuhisa Fujii, Yoshinori Tamai, Toshiki Konishi, and Hiromi Yamakawa*

Department of Polymer Chemistry, Kyoto University, Kyoto 606, Japan

Received July 5, 1990; Revised Manuscript Received September 7, 1990

ABSTRACT: The intrinsic viscosity $[\eta]$ was determined for 22 samples of atactic oligo- and poly(methyl methacrylate)s (a-PMMA), each with the fraction of racemic diads $f_r = 0.79$, in the range of weight-average molecular weight M_w from 3.02×10^2 to 2.83×10^6 in acetonitrile at 44.0 °C (Θ), in *n*-butyl chloride at 40.8 °C (Θ), and in benzene at 30.0 °C. Double-logarithmic plots of $[\eta]$ against M_w for the a-PMMA in the two Θ solvents exhibit inflection with slopes smaller than $^1/_2$ in the range of small M_w, as predicted by the helical wormlike (HW) chain theory. Although the theoretical prediction is only semiquantitative, the HW model parameters determined from an analysis of the data in acetonitrile are rather consistent with those from the mean-square radius of gyration. The values of $[\eta]$ at large M_w in *n*-butyl chloride are found to be ca. 7% larger than those in acetonitrile. It is shown that this difference in $[\eta]$ arises from the difference in the coil limiting value Φ_∞ of the Flory–Fox factor rather than from that in the unperturbed dimension. This is a notion unusual in the field. An analysis of the data in *n*-butyl chloride is also made taking account of the difference in Φ_∞. Further, from a comparison of the results in benzene with those in *n*-butyl chloride, it is shown that the excluded-volume effect occurs at $M_w \simeq 5000$, which corresponds to the reduced contour length equal to ca. 2.9. This result supports again the Yamakawa–Stockmayer–Shimada prediction as in the case of polystyrene.

Introduction

In a previous paper,[1] we have presented some experimental data for the mean-square radius of gyration $\langle S^2 \rangle$ obtained for atactic poly(methyl methacrylate) (a-PMMA) in acetonitrile at 44.0 °C (Θ) using well-characterized oligomer and polymer samples with the fraction of racemic diads $f_r = 0.79$ and shown that the ratio $\langle S^2 \rangle / x_w$ as a function of the weight-average degree of polymerization x_w exhibits a maximum at $x_w \simeq 50$. This has enabled us to rather accurately determine the helical wormlike (HW) model parameters[2,3] for the a-PMMA from an analysis of the data for $\langle S^2 \rangle$ alone, in contrast to the case of atactic polystyrene (a-PS) for which $\langle S^2 \rangle / x_w$ (at Θ) increases monotonically with increasing x_w to its asymptotic value.[4] It has also been shown that this difference between the two polymers arises from the difference in local chain conformation, giving a picture of instantaneous contours of HW Monte Carlo chains generated with the model parameters determined for them.[1]

Now, according to the transport theory of the intrinsic viscosity $[\eta]$ for the HW chain,[5,6] a double-logarithmic plot of $[\eta]$ against the molecular weight M exhibits inflection with a slope smaller than $^1/_2$ in the range of small M for typical cases like a-PMMA. This suggests that we can also determine the HW model parameters for a-PMMA from an analysis of data for $[\eta]$ alone. Indeed, this has already been done with some of the literature data for a- (or syndiotactic) PMMA (at Θ).[6] Thus the main purpose of the present paper is to analyze data for $[\eta]$ obtained for the same a-PMMA samples as used in the previous study[1] and to examine the consistency of the parameters determined here with those from $\langle S^2 \rangle$.

We have already made a similar analysis of the data for $[\eta]$, although in conjunction with the mean-square optical anisotropy $\langle \Gamma^2 \rangle$,[7] obtained for the a-PS ($f_r = 0.59$) in cyclohexane at 34.5 °C (Θ) and in benzene (good solvent) at 25.0 °C,[8] assuming as usual that the unperturbed chain dimension $\langle S^2 \rangle$ may depend on solvent but the Flory–Fox factor Φ (for the unperturbed chain) does not. However, it is clear that there is some doubt about this assumption, especially in the present case. Therefore, we carried out measurements in two Θ solvents and also in a good solvent. In anticipation of results, we claim that, for the present case, the unperturbed Φ depends on solvent but the unperturbed $\langle S^2 \rangle$ does not within experimental error. This then leads to a difficulty in an analysis of the data since there is no available theory of $[\eta]$ that can describe the situation. However, we attempt an analysis by an empirical modification of our theory of $[\eta]$. We also again discuss the onset of the excluded-volume effect on $[\eta]$.

Experimental Section

Materials. Most of the a-PMMA samples used in this work are the same as those used in the study of $\langle S^2 \rangle$,[1] i.e., the fractions separated by gel permeation chromatography (GPC) and/or fractional precipitation from the original samples prepared by group-transfer polymerization for the weight-average molecular weight $M_w \lesssim 3 \times 10^5$ and by radical polymerization for $M_w \gtrsim 3 \times 10^5$. They are sufficiently narrow in molecular weight distribution and have the fraction of racemic diads $f_r = 0.79$ independent of molecular weight, the stereochemical sequences in the chains obeying Bernoullian statistics.[1,9] For the oligomer samples ($M_w < 1.0 \times 10^4$), the values of M_w, the ratio of M_w to the number-average molecular weight M_n, and f_r previously determined[1,9] are reproduced in Table I. (We note that the sample OM3 has not been used previously.[1])

The solvents acetonitrile, *n*-butyl chloride, and benzene used for light scattering (LS) and viscosity measurements were purified according to standard procedures.

Light Scattering. LS measurements were carried out to determine M_w of one additional sample in acetonitrile at 44.0 °C, the Θ temperature of *n*-butyl chloride solutions, M_w of the samples with $M_w > 10^4$ in *n*-butyl chloride at Θ, and $\langle S^2 \rangle$ for the samples with $M_w > 3 \times 10^5$ in *n*-butyl chloride at Θ. For the determination of Θ, the second virial coefficient A_2 was measured for several samples at several temperatures ranging from 30 to 50 °C.

A Fica 50 light scattering photometer was used for all the measurements with vertically polarized incident light of wavelength 436 nm. Scattering intensities were measured for the solutions of five different concentrations and at scattering angles ranging from 30 to 150°. The obtained data were analyzed by an application of the Berry square-root plot.[10]

The most concentrated solutions of the additional sample in acetonitrile and of each sample with $M_w < 3 \times 10^5$ in *n*-butyl chloride were prepared by continuous stirring for 1 day at ca. 50 °C. These solutions and the solvents were optically purified by filtration through an ultracellafilter membrane of pore size 0.45 or 0.1 μm. Preparation of the most concentrated solutions of the samples with $M_w > 3 \times 10^5$ in *n*-butyl chloride required much

0024-9297/91/2224-1608$02.50/0

Table I
Values of M_w, M_w/M_n, and f_r for Atactic Oligo(methyl methacrylate)s

sample	M_w	M_w/M_n	f_r
OM3	302	1.00	0.80
OM4	402	1.00	0.78
OM5	502	1.00	0.78
OM6	602	1.00	
OM7	709	1.00	
OM8	798	1.00	
OM11[a]	1100	1.04	
OM18	1800	1.07	
OM22	2230	1.06	
OM30	2950	1.06	
OM51	5060	1.08	

[a] M_w's of OM11 through OM51 had been determined from LS measurements in acetone at 25.0 °C (see ref 1).

care since their concentrations were changed by filtration. The samples were optically purified by filtration of their acetone solutions through a membrane of pore size 0.45 μm, followed by drying at 50–60 °C for 3 days. The purified samples were dissolved in *n*-butyl chloride optically purified by filtration through a membrane of pore size 0.1 μm. The solutions were allowed to stand in the dark at 50 °C for 1 day and then stirred gently for 1 h just before measurement. All the solutions of lower concentrations were obtained by sequential dilution. The weight concentrations of test solutions were determined gravimetrically and converted to mass concentrations by using the densities of the solutions.

The refractive index increment $\partial n/\partial c$ was measured at 436 nm for the a-PMMA sample with $M_w = 1.19 \times 10^5$ in *n*-butyl chloride at 40.8 °C by the use of a Shimadzu differential refractometer. The value of $\partial n/\partial c$ was 0.099 cm³/g.

Viscosity. Viscosity measurements were carried out for 22 and 21 a-PMMA samples in acetonitrile at 44.0 °C (Θ) and in *n*-butyl chloride at 40.8 °C (Θ) (see the Results section), respectively, and for 15 samples in benzene at 30.0 °C. For the measurements, we used a viscometer of the Ubbelohde type and two specially designed (four-bulb) spiral capillary viscometers of the suspended-liquid type having long flow times. We note that the longest flow times of pure acetonitrile (44.0 °C), *n*-butyl chloride (40.8 °C), and benzene (30.0 °C) are about 1460, 1630, and 2520 s, respectively, for one of the spiral capillary viscometers and about 630, 700, and 1080 s, respectively, for the other. (The latter had been used in the study of [η] of the oligostyrenes.[8]) These three viscometers were appropriately used so that the specific viscosity η_{sp} was accurately determined in the range from 0.01 to 0.1. The actual measurements were carried out at polymer concentrations corresponding to values of η_{sp} ranging from 0.01 to 0.1. The flow time was measured to a precision of 0.1 s, and each test solution was maintained at constant temperature within ±0.005 °C during the measurements.

The polymer mass concentration *c* of the solution was varied in the range from 0.0002 to 0.04 g/cm³. Density corrections were made in the calculations of *c* and also of the relative viscosity η_r from the flow times of the solution and solvent. The solution density was measured as a function of the weight fraction and M_w with a picnometer of the Lipkin–Davison type.

The obtained data for η_{sp} and η_r for each sample were treated as usual by the Huggins and Fuoss–Mead plots to evaluate [η].

Results

Light Scattering. The values of M_w determined for the a-PMMA samples with $M_w > 10^4$ in the two solvents acetonitrile and *n*-butyl chloride (at the respective Θ) are given in Table II along with the values of M_w/M_n and f_r. We note that the values of M_w in acetonitrile and of M_w/M_n except for the additional sample MM22 and all the values of f_r have been reproduced from the previous paper[1] and that the samples MM6′ ($M_w = 6.09 \times 10^4$) and MM12″ ($M_w = 1.21 \times 10^5$), which were used only for the determination of Θ, are omitted in the table. The value of M_w for each sample determined in *n*-butyl chloride is in good

Table II
Values of M_w, M_w/M_n, and f_r for Atactic Poly(methyl methacrylate)s

sample	M_w		M_w/M_n	f_r
	acetonitrile	*n*-butyl chloride		
MM1	1.09×10^4	1.09×10^4	1.06	
MM2	1.90×10^4	1.88×10^4	1.08	
MM4	3.53×10^4	3.50×10^4	1.07	
MM5	5.16×10^4	4.84×10^4	1.07	0.78
MM7	7.40×10^4	7.35×10^4	1.09	
MM12	1.19×10^5	1.18×10^5	1.09	
MM22	2.18×10^5	2.15×10^5	1.06	
Mr4	3.61×10^5	3.47×10^5	1.07	
Mr8	7.58×10^5	7.83×10^5	1.05	0.79
Mr19	1.90×10^6	1.98×10^6	1.06	
Mr28	2.83×10^6	2.83×10^6	1.10	0.79

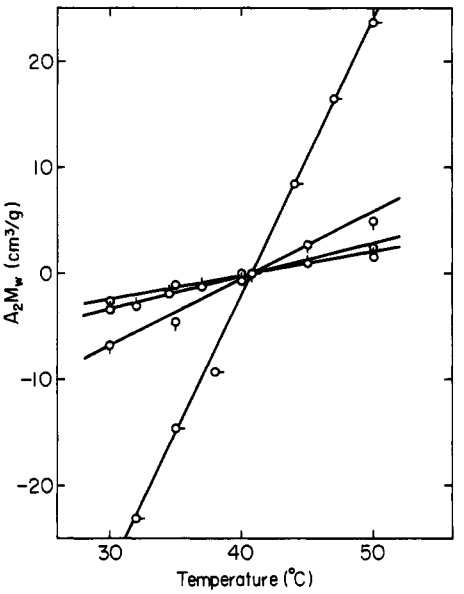

Figure 1. Plots of A_2M_w against temperature for a-PMMA samples with $f_r = 0.79$ in *n*-butyl chloride: (○) MM5, (◔) MM6′ ($M_w = 6.09 \times 10^4$); (◕) MM12″ ($M_w = 1.21 \times 10^5$); (●) Mr8.

agreement with that in acetonitrile and also with that determined in acetone in the previous study.[1] Recall that the values of M_w in acetonitrile and in acetone agreed well with each other. This indicates that there occurs no possible molecular association in *n*-butyl chloride as well as in acetonitrile provided that the solutions are dilute. (The value of M_w/M_n for the sample MM22 from the GPC analysis confirms that its molecular weight distribution is also sufficiently narrow.)

Figure 1 shows plots of A_2M_w against temperature for the four samples MM5, MM6′, MM12″, and Mr8. It is seen that A_2 vanishes at the same temperature independent of M_w provided that $M_w \gtrsim 5 \times 10^4$. Thus this leads to the conclusion that the Θ temperature is 40.8 °C for *n*-butyl chloride solutions of a-PMMA with $f_r = 0.79$. (As shown later, A_2 in fact vanishes in *n*-butyl chloride at 40.8 °C also for the samples Mr4, Mr19, and Mr28 for which we carried out LS measurements of $\langle S^2 \rangle$.) This value of Θ is somewhat higher than the value ~34 °C determined by Schulz and Kirste,[11] and this is discussed below.

The excess reduced scattering intensities ΔR_{Uv} measured with vertically polarized incident light and without an analyzer for the samples Mr4, Mr8, Mr19, and Mr28 in *n*-butyl chloride at the Θ determined above were analyzed by an application of the Berry square-root plot in order to determine $\langle S^2 \rangle$. The values of $(Kc/\Delta R_{Uv})_{\theta=0}^{1/2}$ and $(Kc/\Delta R_{Uv})_{c=0}^{1/2}$ with *K* the optical constant were determined from the square-root plots of the data for $Kc/\Delta R_{Uv}$

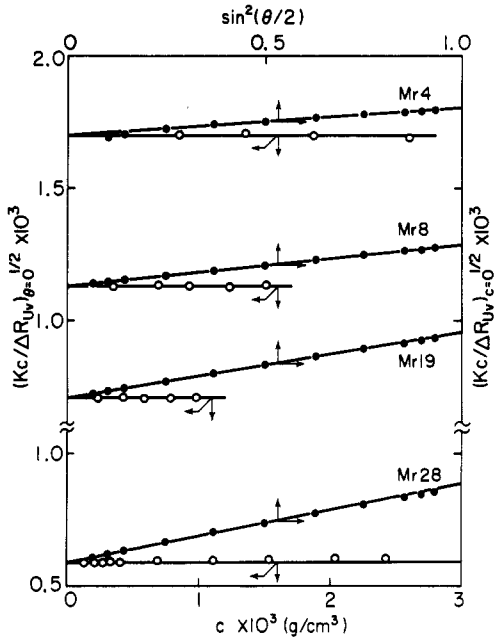

Figure 2. Plots of $(Kc/\Delta R_{Uv})_{\theta=0}^{1/2}$ against c (○) and $(Kc/\Delta R_{Uv})_{c=0}^{1/2}$ against $\sin^2(\theta/2)$ (●) for the a-PMMA samples indicated in *n*-butyl chloride at 40.8 °C.

Table III
Values of $\langle S^2\rangle^{1/2}$ and $\langle S^2\rangle/M_w$ for Atactic Poly(methyl methacrylate)s in *n*-Butyl Chloride at 40.8 °C (Θ)

sample	$10^{-2}\langle S^2\rangle^{1/2}$, Å	$10^2\langle S^2\rangle/M_w$, Å²	sample	$10^{-2}\langle S^2\rangle^{1/2}$, Å	$10^2\langle S^2\rangle/M_w$, Å²
Mr4	1.5_0	6.4_8	Mr19	3.5_8	6.4_7
Mr8	2.2_6	6.5_2	Mr28	4.3_1	6.5_6

at finite scattering angles θ and concentrations c by extrapolation to zero angle and zero concentration, respectively. The results are plotted against c and $\sin^2(\theta/2)$, respectively, in Figure 2. It is seen that all the plots of $(Kc/\Delta R_{Uv})_{\theta=0}^{1/2}$ against c follow horizontal straight lines for $c \lesssim 5 \times 10^{-4}$ g/cm³, indicating that A_2 vanishes for each sample. It should be noted here that the data points for the sample Mr28 for $c \gtrsim 5 \times 10^{-4}$ g/cm³ deviate upward from the corresponding horizontal straight line and therefore that a determination of A_2 with high M_w becomes inaccurate unless the concentrations are sufficiently low. The disagreement between the Θ temperatures determined by Schulz and Kirste[11] and by us may be due to the fact that they indeed obtained data over a wider concentration range, which give the apparent vanishing of A_2 at their Θ lower than ours.

The values of $\langle S^2\rangle$ of the four samples above have been determined from the slopes of the plots $(Kc/\Delta R_{Uv})_{c=0}^{1/2}$ against $\sin^2(\theta/2)$ and the common intercepts of the two kinds of plots. The results are given in Table III along with the values of $\langle S^2\rangle/M_w$. The latter values are in good agreement with the value $6.6_6 \times 10^{-2}$ Å² obtained for the a-PMMA in acetonitrile at Θ as the mean of the values for the samples Mr4, Mr8, Mr19, and Mr28.[1] Thus we may conclude that the unperturbed dimensions of the a-PMMA are almost the same in these two Θ solvents.

Viscosity. Intrinsic viscosity data for the a-PMMA samples listed in Tables I and II in the two Θ solvents and in benzene are summarized in Table IV along with the values of the Huggins coefficient k'. Except in the very oligomer region, the values of k' in acetonitrile are somewhat greater than those in *n*-butyl chloride, both of them being greater than the values for the a-PS in cyclohexane at 34.5 °C (Θ)[8,12] (for $M_w \gtrsim 10^4$).

Table IV
Results of Viscometry on Atactic Oligo- and Poly(methyl methacrylate)s in Acetonitrile at 44.0 °C, in *n*-Butyl Chloride at 40.8 °C, and in Benzene at 30.0 °C

	acetonitrile (44.0 °C)		*n*-butyl chloride (40.8 °C)		benzene (30.0 °C)	
sample	$[\eta]$, dL/g	k'	$[\eta]$, dL/g	k'	$[\eta]$, dL/g	k'
OM3	0.0143	1.1	0.0168	0.92	0.0174	0.63
OM4	0.0168	1.1	0.0201	0.96	0.0215	0.87
OM5	0.0189	1.0	0.0224	1.2	0.0241	0.84
OM6	0.0209	0.93	0.0248	0.99	0.0268	0.81
OM7	0.0221	1.1	0.0262	1.0	0.0280	0.96
OM8	0.0236	0.89	0.0285	0.99	0.0299	0.95
OM11	0.0270	0.83	0.0309	1.1	0.0329	0.94
OM18	0.0357	0.93	0.0398	0.58	0.0407	0.98
OM22	0.0390	0.93	0.0435	0.54	0.0444	0.80
OM30	0.0422	0.78	0.0471	0.50	0.0480	0.89
OM51	0.0508	0.83	0.0601	0.56	0.0635	0.69
MM1	0.0673	1.0	0.0750	0.64	0.0950	0.50
MM2	0.0830	1.0	0.0916	1.0		
MM4	0.106	1.1	0.121	0.85	0.200	0.33
MM5	0.124	0.96	0.139	0.90		
MM7	0.150	1.0	0.166	0.86		
MM12	0.194	1.1	0.200	0.98	0.447	0.40
MM22	0.253	1.1	0.277	0.97		
Mr4	0.333	0.95	0.341	0.80		
Mr8	0.473	1.2	0.527	0.73	1.58	0.33
Mr19	0.784	1.1				
Mr28	0.962	1.1	1.00	0.67		

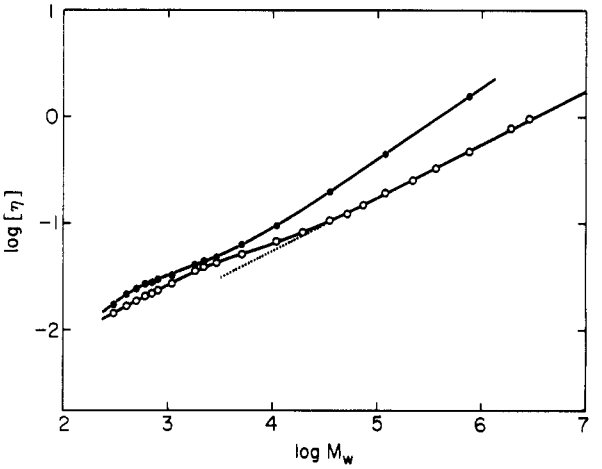

Figure 3. Double-logarithmic plots of $[\eta]$ (in dL/g) against M_w for a-PMMA with $f_r = 0.79$: (○) in acetonitrile at 44.0 °C; (●) in benzene at 30.0 °C. The dotted straight line has a slope of 0.5.

In Figure 3 are shown double-logarithmic plots of $[\eta]$ (in dL/g) against M_w for the data in acetonitrile at 44.0 °C (unfilled circles) and in benzene at 30.0 °C (filled circles). The solid curves connect the data points smoothly, and the dotted line indicates an asymptotic straight line of slope $^1/_2$ for the data in acetonitrile. We note that the values of M_w used for these plots are those listed in Table I (for $M_w < 10^4$) and those in the second column of Table II (in acetonitrile). Figure 4 shows similar plots for the data in *n*-butyl chloride at 40.8 °C. The solid curve connects the data points smoothly, the dotted line indicates its asymptotic straight line of slope $^1/_2$ as in Figure 3, and the dashed and dot-dashed curves have been reproduced from the corresponding curves in Figure 3 for the data in acetonitrile and in benzene, respectively. For the plot of the data in *n*-butyl chloride in Figure 4, we have used the values of M_w listed in the third column of Table III (in this solvent) for $M_w > 10^4$.

As was expected from the behavior of $\langle S^2\rangle/x_w$,[1] both plots of the data in the two Θ solvents clearly exhibit inflection, following the respective asymptotic straight

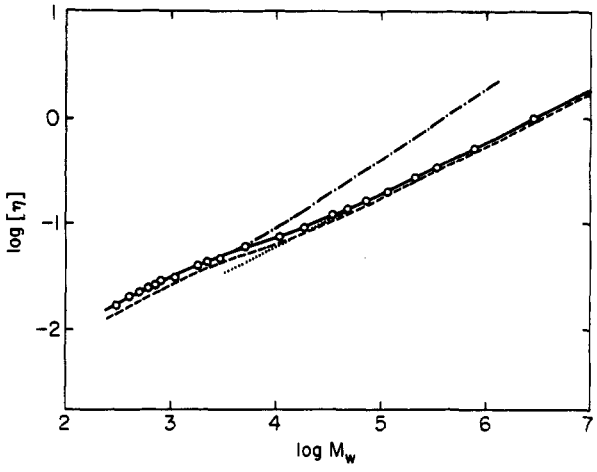

Figure 4. Double-logarithmic plots of $[\eta]$ (in dL/g) against M_w for a-PMMA with $f_r = 0.79$ in *n*-butyl chloride at 40.8 °C. The dashed and dot-dashed curves represent the experimental results for the a-PMMA in acetonitrile at 44.0 °C and in benzene at 30.0 °C, respectively (see Figure 3), and the dotted straight line has a slope of 0.5.

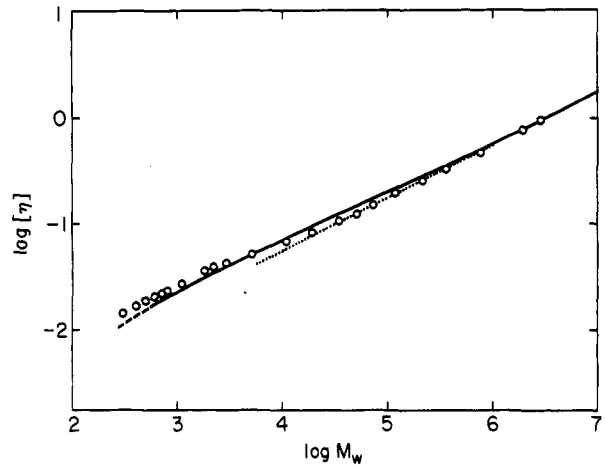

Figure 5. Comparison between the observed and theoretical values of $[\eta]$ (in dL/g) for the a-PMMA in acetonitrile at 44.0 °C. The solid curve represents the best fit HW theoretical values for $N \geq 2$, the dashed line segment connecting the values for $N = 1$ and 2. The dotted straight line has a slope of 0.5.

lines of slope $^1/_2$ for $M_w \gtrsim 6 \times 10^4$ in acetonitrile and for $M_w \gtrsim 10^5$ in *n*-butyl chloride, whose ranges start at higher M_w than those in the case of the a-PS in cyclohexane at 34.5 °C. It is interesting to note that the values of $[\eta]$ in *n*-butyl chloride are somewhat (more than 7%) larger than those in acetonitrile over the whole range of M_w studied despite the agreement between the unperturbed dimensions in the two solvents mentioned above. The plot of the data in benzene almost agrees with that in *n*-butyl chloride for $M_w \lesssim 5 \times 10^3$, but the former deviates upward from the latter for large M_w because of the excluded-volume effect.

Discussion

HW Model Parameters. Before proceeding to make an analysis of the present data for $[\eta]$ on the basis of the HW model, it is convenient here to give a brief description of its parameters.[2] All the equilibrium conformational properties of the HW chain may be described by the four basic model parameters: the differential geometrical curvature κ_0 and torsion τ_0 of the characteristic regular helix, which the HW chain contour takes at the minimum zero of its total elastic energy, the static stiffness parameter λ^{-1} as defined as the bending force constant divided by $k_BT/2$ with k_B the Boltzmann constant and T the absolute temperature, and the shift factor M_L as defined as the molecular weight per unit contour length. However, in order to treat its transport coefficients, it is necessary to introduce an additional parameter describing the hydrodynamic thickness of a given polymer chain, i.e., the bead diameter d_b for the touched-bead model[6] or the cylinder diameter d for the cylinder model.[5] Recall that the two hydrodynamic parameters d_b and d are related to each other by the relation $d = 0.74d_b$ as far as $[\eta]$ is concerned.[6]

Now, the intrinsic viscosity $[\eta]$ of the HW touched-bead model with the total number N of beads or of the total contour length $L = Nd_b$ may be written, in terms of the parameters defined above, as follows

$$[\eta] = (1/\lambda^2 M_L) f_\eta(\lambda L; \lambda^{-1}\kappa_0, \lambda^{-1}\tau_0, \lambda d_b) \quad (1)$$

The function f_η is defined by

$$f_\eta(\lambda L) = \lambda^{-1} M_L [\bar{\eta}] \quad (2)$$

where $[\bar{\eta}]$ is the intrinsic viscosity measured in units of $(\lambda^{-1})^3$ and is given by eq 15 with eqs 17 and 27 of ref 6. The function f_η satisfies the asymptotic relation

$$\lim_{\lambda L \to \infty} f_\eta(\lambda L)/(\lambda L)^{1/2} = c_\infty^{3/2} \Phi_\infty \quad (3)$$

with

$$c_\infty = \frac{4 + (\lambda^{-1}\tau_0)^2}{4 + (\lambda^{-1}\kappa_0)^2 + (\lambda^{-1}\tau_0)^2} \quad (4)$$

and with Φ_∞ ($=2.870 \times 10^{23}$ mol^{-1}) the coil limiting value of the Flory–Fox factor Φ (see below). As was done in previous studies,[5,6,8] we consider double-logarithmic plots of $[\eta]$ against M by the use of the equations[5]

$$\log [\eta] = \log f_\eta(\lambda L; \lambda^{-1}\kappa_0, \lambda^{-1}\tau_0, \lambda d_b) - \log (\lambda^2 M_L) \quad (5)$$

$$\log M = \log (\lambda L) + \log (\lambda^{-1} M_L) \quad (6)$$

The quantities $\lambda^2 M_L$ and $\lambda^{-1} M_L$ (and therefore λ^{-1} and M_L) may be estimated from a best fit of double-logarithmic plots of the theoretical f_η against λL for properly chosen values of $\lambda^{-1}\kappa_0$, $\lambda^{-1}\tau_0$, and λd_b to that of the observed $[\eta]$ against M_w, so that we may determine $\lambda^{-1}\kappa_0$, $\lambda^{-1}\tau_0$, λ^{-1}, M_L, and d_b.

Figure 5 shows double-logarithmic plots of $[\eta]$ against M for the a-PMMA in acetonitrile at 44.0 °C. The unfilled circles represent the experimental values, and the solid curve represents the best fit theoretical values for $N \geq 2$ calculated from eq 1 with $\lambda^{-1}\kappa_0 = 4.5$, $\lambda^{-1}\tau_0 = 2.0$, $\lambda d_b = 0.16$, $\log (\lambda^2 M_L) = -1.72$, and $\log (\lambda^{-1} M_L) = 3.24$, the dashed line segment connecting those values for $N = 1$ and 2. The dotted line indicates an asymptotic straight line of slope $^1/_2$. The values of the HW model parameters thus determined are listed in the first row of Table V along with those determined from an analysis of $\langle S^2 \rangle$ for the same system[1] and those for the a-PS in cyclohexane at 34.5 °C.[8] We note that the HW chain with $\lambda^{-1}\kappa_0 = 4.5$ and $\lambda^{-1}\tau_0 = 2.0$ does not exhibit a maximum in the ratio $\langle S^2 \rangle / x_w$ as a function of x_w as observed experimentally.[1] Thus the parameters determined from the analysis of $[\eta]$ are not consistent with those from $\langle S^2 \rangle$ in that sense. However, both values of λ^{-1} are definitely larger than that for the a-PS, and both sets of values of the parameters $\lambda^{-1}\kappa_0$ and $\lambda^{-1}\tau_0$ indicate that the a-PMMA chain is of strong helical nature. (The term "strong helical nature" means that the chain contour retains large helical portions even with thermal fluctuations. Quantitatively, such a chain

Table V
Values of the HW Model Parameters

polymer (f_r)	solvent	temp, °C	$\lambda^{-1}\kappa_0$	$\lambda^{-1}\tau_0$	λ^{-1}, Å	M_L, Å^{-1}	d_b, Å	obsd quantity
a-PMMA (0.79)	acetonitrile	44.0	4.5	2.0	45.0	38.6	7.2	$[\eta]$
	n-butyl chloride	40.8	(4.5)	(2.0)	(45.0)	(38.6)	7.9	$[\eta]$
	acetonitrile	44.0	4.0	1.1	57.9	36.3		$\langle S^2\rangle$
a-PS (0.59)	cyclohexane	34.5	3.0	6.0	23.5	42.6	10.1	$\langle\Gamma^2\rangle$, $[\eta]$

Table VI
Values of $\langle S^2\rangle^{1/2}$ and Φ for Atactic Oligo- and Poly(methyl methacrylate)s in Acetonitrile at 44.0 °C

sample	$\langle S^2\rangle^{1/2}$, Å	$10^{-23}\Phi$, mol^{-1}	sample	$\langle S^2\rangle^{1/2}$, Å	$10^{-23}\Phi$, mol^{-1}
OM4	2.9_7[a]	$17._5$	MM1	$27._6$	2.3_7
OM5	3.7_5	$12._2$	MM2	$35._4$	2.4_2
OM6	4.3_0	$10._8$	MM4	$48._0$	2.3_0
OM7	5.4_1	6.7_3	MM5	$56._4$	2.4_3
OM8	5.8_3	6.4_7	MM7	$68._9$	2.3_1
OM11	7.4_9	4.8_1	MM12	$87._5$	2.3_4
OM18	$10._9$	3.3_8	Mr4	15_6	2.1_5
OM22	$12._3$	3.1_8	Mr8	22_4	2.1_7
OM30	$14._1$	3.0_2	Mr19	35_4	2.2_8
OM51	$18._9$	2.5_9	Mr28	43_5	2.2_5

[a] Reproduced from ref 1.

Table VII
Values of Φ for Atactic Poly(methyl methacrylate) in *n*-Butyl Chloride at 40.8 °C

sample	$10^{-23}\Phi$, mol^{-1}	sample	$10^{-23}\Phi$, mol^{-1}
Mr4	2.3_9	Mr28	2.4_1
Mr8	2.4_3		

has $\lambda^{-1}\kappa_0 \gtrsim 2$ and $\lambda^{-1}\tau_0 \lesssim \lambda^{-1}\kappa_0/\pi$.[13] Thus we may say that the two sets of the model parameters are rather consistent with each other.

As seen from Figure 5, the theoretical curve reproduces only qualitatively the inverse S-shaped one experimentally observed, the curvature of the former being weaker than that of the latter. In other words, the experimental data follow the asymptotic straight line at a smaller value of M_w than do the theoretical values. It is also seen that the single bead of the HW touched-bead model corresponds to three monomer units. This should be compared with the case of the a-PS, for which the single bead corresponds to four monomer units,[8] and the agreement between theory and experiment in the very oligomer region is worse.

Flory–Fox Factor Φ. As in the previous study of the a-PS chain,[4] we have calculated the Flory–Fox factor Φ from the relation

$$[\eta] = 6^{3/2}\Phi\langle S^2\rangle^{3/2}/M \tag{7}$$

in order to discuss the present results for $[\eta]$ in connection with the previous ones for $\langle S^2\rangle$.[1] The results for the acetonitrile solutions are given in Table VI along with the values of $\langle S^2\rangle^{1/2}$ determined previously,[1] and those for the *n*-butyl chloride solutions are also given in Table VII, for comparison. For the latter, we have obtained the values of Φ only for the samples with sufficiently high M_w, since $\langle S^2\rangle$ for the samples with low M_w could not be determined from small-angle X-ray scattering measurements.[1]

The coil limiting value Φ_∞ of Φ in acetonitrile has been calculated to be $2.2_1 \times 10^{23}$ mol^{-1} as the mean of the values of Φ for the samples Mr4, Mr8, Mr19, and Mr28 listed in Table VI and that in *n*-butyl chloride to be $2.4_1 \times 10^{23}$ mol^{-1} as the mean of the values listed in Table VII. The former value is appreciably smaller than the latter. On the other hand, the coil limiting values of the ratio $\langle S^2\rangle/M_w$ are $6.6_8 \times 10^{-2}$ Å^2 in acetonitrile, as mentioned before, and $6.5_1 \times 10^{-2}$ Å^2 in *n*-butyl chloride as the mean of the values listed in Table III, and they may be regarded as nearly identical with each other within experimental error. Thus it may be said that the difference between the coil limiting values of the ratio $[\eta]/M_w^{1/2}$ for the two solutions mentioned in the Results section arises from the difference in Φ_∞ rather than from that in $\langle S^2\rangle/M_w$. Note that according to the prevailing notion for the unperturbed (Θ) chain, Φ_∞ is a universal constant.

Now, the calculation of the HW theoretical values of Φ requires the theoretical values of $\langle S^2\rangle$. For the HW chain of total contour length L, $\langle S^2\rangle$ is given by[2,3]

$$\langle S^2\rangle = \lambda^{-2} f_S(\lambda L; \lambda^{-1}\kappa_0, \lambda^{-1}\tau_0) \tag{8}$$

where the function f_S is defined by

$$f_S(\lambda L; \lambda^{-1}\kappa_0, \lambda^{-1}\tau_0) = \frac{\tau_0^2}{\lambda^2\nu^2} f_{S,KP}(\lambda L) + \frac{\kappa_0^2}{\lambda^2\nu^2}\left[\frac{\lambda L}{3r}\cos\phi - \frac{1}{r^2}\cos(2\phi) + \frac{2}{r^3\lambda L}\cos(3\phi) - \frac{2}{r^4\lambda^2 L^2}\cos(4\phi) + \frac{2}{r^4\lambda^2 L^2}e^{-2\lambda L}\cos(\nu\lambda L + 4\phi)\right] \tag{9}$$

with

$$\nu = (\lambda^{-2}\kappa_0^2 + \lambda^{-2}\tau_0^2)^{1/2} \tag{10}$$

$$r = (4 + \nu^2)^{1/2} \tag{11}$$

$$\phi = \cos^{-1}(2/r) \tag{12}$$

and

$$f_{S,KP}(\lambda L) = \frac{\lambda L}{6} - \frac{1}{4} + \frac{1}{4\lambda L} - \frac{1}{8\lambda^2 L^2}(1 - e^{-2\lambda L}) \tag{13}$$

We note that f_S satisfies the asymptotic relation

$$\lim_{\lambda L\to\infty} f_S(\lambda L)/\lambda L = \frac{1}{6}c_\infty \tag{14}$$

and that eq 8 with eq 9 gives $\langle S^2\rangle$ for the Kratky–Porod wormlike chain[14] when $\kappa_0 = 0$. As mentioned above, the theoretical value of Φ_∞ (calculated from eq 7 with eqs 1 and 8) is the universal constant 2.870×10^{23} mol^{-1}, but it differs appreciably from the experimental values above. Thus, for a comparison between theory and experiment regarding the dependence of Φ on M, we multiply the theoretical Φ by the constant ratio of the experimental to the theoretical Φ_∞, for convenience.

Figure 6 shows double-logarithmic plots of Φ against M_w. The unfilled circles represent the experimental values in acetonitrile, and the solid curve represents the corresponding theoretical values calculated by the above procedure with the HW model parameters listed in the first row of Table V. As in the case of the a-PS in cyclohexane at 34.5 °C,[4] the observed Φ is substantially constant for M_w higher than 10^5 but steeply increases as M_w is decreased from 10^5. The theory may explain such behavior semiquantitatively; the agreement with experiment is not so good as in the case of the a-PS.[4] This is due to the fact that the theoretical values of $\langle S^2\rangle$ calculated with the model parameters determined from $[\eta]$ fail to

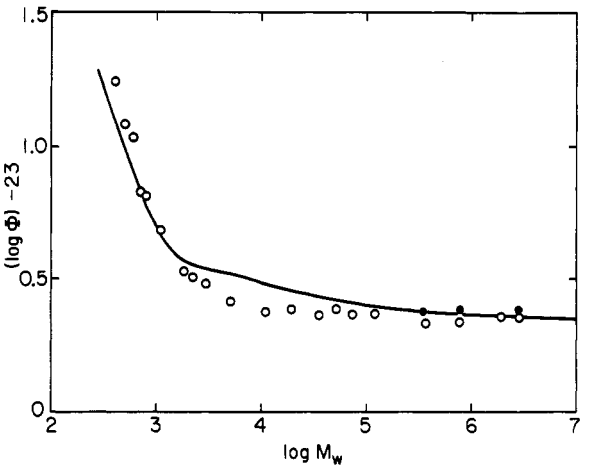

Figure 6. Molecular weight dependence of the Flory–Fox factor Φ for a-PMMA with $f_r = 0.79$: (○) in acetonitrile at 44.0 °C; (●) in *n*-butyl chloride at 40.8 °C. Solid curve, the HW theoretical values calculated with $\lambda^{-1}\kappa_0 = 4.5$, $\lambda^{-1}\tau_0 = 2.0$, $\lambda^{-1} = 45.0$ Å, $M_L = 38.6$ Å^{-1}, and $d_b = 7.9$ Å (see the text).

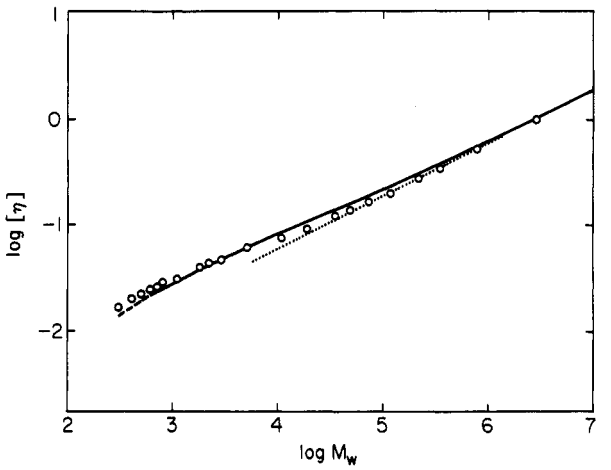

Figure 7. Comparison between the observed and theoretical values of $[\eta]$ (in dL/g) for the a-PMMA in *n*-butyl chloride at 40.8 °C. The solid curve represents the best fit HW theoretical values for $N \geq 2$, the dashed line segment connecting the values for $N = 1$ and 2 (see the text). The dotted straight line has a slope of 0.5.

well reproduce the experimental values[1] in the range of $2 \times 10^3 \lesssim M_w \lesssim 3 \times 10^4$. In Figure 6 are also shown the experimental values of Φ in *n*-butyl chloride (filled circles), which are appreciably larger than the values in acetonitrile, as mentioned above.

Solvent Effects on the Unperturbed Chain. As mentioned in the preceding subsection, the observed value Φ_∞ in *n*-butyl chloride is appreciably larger than that in acetonitrile. In this connection, it is pertinent here to refer to the previous analysis of the data for $[\eta]$ for the a-PS in cyclohexane at 34.5 °C and in benzene at 25.0 °C.[8] In that case, we have attributed the difference between $[\eta]/M_w^{1/2}$ in the unperturbed states in these solvents to that between the unperturbed dimensions $\langle S^2 \rangle$, assuming that Φ_∞ is independent of solvent. However, this assumption is no longer valid since it has been proved that Φ_∞ is dependent on solvent but $\langle S^2 \rangle$ is not in the present case.

This dependence of Φ_∞ on solvent requires some consideration in an analysis of the data in *n*-butyl chloride, since any existent theory of $[\eta]$ cannot explain this fact. Here we use a maneuver to remove the difficulty, i.e., introduce empirically a constant prefactor C_η into the right-hand side of eq 1 as

$$[\eta] = (C_\eta/\lambda^2 M_L) f_\eta \tag{15}$$

in order to interpret the difference between Φ_∞ in the two Θ solvents, where C_η is set equal to the ratio of Φ_∞ in *n*-butyl chloride to that in acetonitrile, 1.09.

Figure 7 shows double-logarithmic plots of $[\eta]$ against M for the a-PMMA in *n*-butyl chloride at 40.8 °C. The unfilled circles represent the experimental values. Since the unperturbed dimensions in the two solvents are the same, the local chain conformations may also be considered so. Thus it is reasonable to assume that the static model parameters $\lambda^{-1}\kappa_0$, $\lambda^{-1}\tau_0$, λ^{-1}, and M_L are the same in the two solvents but the hydrodynamic parameter d_b is not. In the figure, the solid curve represents the best fit theoretical values for $N \geq 2$ thus calculated from eq 15 with $\lambda d_b = 0.175$, the dashed line segment connecting those values for $N = 1$ and 2. The value of d_b thus determined is given in the second row of Table V, and it is somewhat larger than that in acetonitrile. As in the case of the acetonitrile solutions, the theoretical curve reproduces only qualitatively the inverse S-shaped one experimentally observed.

Excluded-Volume Effects. Now, we discuss the onset of the excluded-volume effect. Apart from values of Φ_∞ and $\langle S^2 \rangle$, the values of $[\eta]$ in benzene and in *n*-butyl chloride are almost identical with each other in the oligomer region, as seen from Table IV or Figure 4. Thus the values of $[\eta]$ in *n*-butyl chloride may be regarded as the unperturbed values of $[\eta]$ in benzene.

It is seen from Figure 4 that the excluded-volume effect begins to occur at $M_w \simeq 5000$, at which the dot-dashed and solid curves separate from each other. This value of M_w corresponds to the value 10.2 of the number of Kuhn statistical segments $n_K = M/M_L A_K$ with A_K the Kuhn statistical segment length given by

$$A_K = c_\infty \lambda^{-1} \tag{16}$$

This critical value of n_K, which has been calculated with the model parameters listed in the second row of Table V, is much smaller than the value of 50 estimated by Norisuye and Fujita[15] but is appreciably larger than the value of 6.5 determined previously[8] for a-PS. However, the critical values of the reduced contour length $\lambda L = \lambda M/M_L$ are 2.9 and 5.5 for a-PMMA and a-PS, respectively, and both are consistent with the Yamakawa–Stockmayer–Shimada theory prediction[16,17] or the Monte Carlo simulation results for the rotational isomeric state chain by Yamakawa and Shimada.[18]

Concluding Remarks

We have been able to determine rather unambiguously the HW model parameters for the a-PMMA (with $f_r = 0.79$) from an analysis of the data for $[\eta]$ alone in acetonitrile at 44.0 °C (Θ). Their values determined may be regarded as consistent with those from $\langle S^2 \rangle$ in the sense that the former indicates as well as the latter that the a-PMMA chain is of strong helical nature. However, the agreement between the parameters from the two properties is not very good compared with the case of the a-PS.[4,8] (The agreement between theory and experiment for $[\eta]$ in the very oligomer region is better for the a-PMMA.) Indeed, the present parameters for the a-PMMA from $[\eta]$ can only reproduce semiquantitatively the inverse S-shaped curve followed by its double-logarithmic plot against M_w or the behavior of the Flory–Fox factor Φ and fail to predict the maximum in $\langle S^2 \rangle / x_w$ as a function of x_w. This implies that the HW transport theory does not work very well in the case of the chain of strong helical nature. Thus we prefer the model parameters for the a-PMMA from $\langle S^2 \rangle$ to those from $[\eta]$.

We have found that the coil limiting value Φ_∞ of Φ depends definitely on solvent in the present case. In this connection, it is important to note that we have recently predicted on the basis of the HW chain that the (unperturbed) ratio ρ of the hydrodynamic radius R_H from the translational diffusion coefficient to $\langle S^2 \rangle^{1/2}$ may depend not only on the local chain conformation but also on the hydrodynamic chain thickness if the Oseen hydrodynamic interaction tensor is not preaveraged.[19] This will probably be the case with Φ_∞. Thus we are now pursuing a precise experimental study of ρ and Φ_∞ for a variety of polymer–Θ-solvent systems.

Acknowledgment. We thank Drs. Y. Einaga and T. Yoshizaki for their assistance. This research was supported in part by a Grant-in-Aid (01430018) from the Ministry of Education, Science, and Culture, Japan.

References and Notes

(1) Tamai, Y.; Konishi, T.; Einaga, Y.; Fujii, M.; Yamakawa, H. *Macromolecules* **1990**, *23*, 4067.
(2) Yamakawa, H. *Annu. Rev. Phys. Chem.* **1984**, *35*, 23.
(3) Yamakawa, H.; Fujii, M. *J. Chem. Phys.* **1976**, *64*, 5222.
(4) Konishi, T.; Yoshizaki, T.; Saito, T.; Einaga, Y.; Yamakawa, H. *Macromolecules* **1990**, *23*, 290.
(5) Yamakawa, H.; Yoshizaki, T. *Macromolecules* **1980**, *13*, 633.
(6) Yoshizaki, T.; Nitta, I.; Yamakawa, H. *Macromolecules* **1988**, *21*, 165.
(7) Konishi, T.; Yoshizaki, T.; Shimada, J.; Yamakawa, H. *Macromolecules* **1989**, *22*, 1921.
(8) Einaga, Y.; Koyama, H.; Konishi, T.; Yamakawa, H. *Macromolecules* **1989**, *22*, 3419.
(9) Konishi, T.; Tamai, Y.; Fujii, M.; Einaga, Y.; Yamakawa, H. *Polym. J. (Tokyo)* **1989**, *21*, 329.
(10) Berry, G. C. *J. Chem. Phys.* **1966**, *44*, 4550.
(11) Schulz, G. V.; Kirste, R. *Z. Phys. Chem. (Neue Folge)* **1961**, *30*, 171.
(12) Einaga, Y.; Miyaki, Y.; Fujita, H. *J. Polym. Sci., Polym. Phys. Ed.* **1979**, *17*, 2103.
(13) Yamakawa, H.; Shimada, J.; Fujii, M. *J. Chem. Phys.* **1978**, *68*, 2140.
(14) Benoit, H.; Doty, P. *J. Phys. Chem.* **1953**, *57*, 958.
(15) Norisuye, T.; Fujita, H. *Polym. J. (Tokyo)* **1982**, *14*, 143.
(16) Yamakawa, H.; Stockmayer, W. H. *J. Chem. Phys.* **1972**, *57*, 2843.
(17) Shimada, J.; Yamakawa, H. *J. Chem. Phys.* **1986**, *85*, 591.
(18) Yamakawa, H.; Shimada, J. *J. Chem. Phys.* **1985**, *83*, 2607.
(19) Yamakawa, H.; Yoshizaki, T. *J. Chem. Phys.* **1989**, *91*, 7900.

Registry No. PMMA (homopolymer), 9011-14-7; acetonitrile, 75-05-8; *n*-butyl chloride, 109-69-3; benzene, 71-43-2.